Class-D Amplifier-Based Core Loss Measurements for High Frequency Magnetic Materials

Jacob R. Anderson, Nick J. Kirkby, Mike K. Ranjram Miniaturized and Advanced Power Electronics Laboratory Arizona State University Email: {jrande39, njk, mranjram}@asu.edu

Abstract—Magnetic core loss measurement methods suitable for high-frequency sinusoidal excitations are currently time intensive or inherently suffer from flux drive limitations due to the costly and ill-suited radio frequency (RF) equipment utilized in the measurement. The recent development of automated testers has enabled the collection of large core loss data sets across a broad range of operating frequencies and flux densities. Improper loading of the RF power amplifiers utilized in these measurements makes the collection of accurate core loss data impractical above certain drive levels. In this paper, we develop and demonstrate an automatable core loss testing method which replaces the commonly employed RF power amplifier with a high frequency switching inverter. An analytical framework for assessing flux harmonics in the core is also presented. An experimental demonstration is perforned in the range of 1-7MHz for the following materials: (1) Fair-Rite 67, (2) Fair-Rite 80, and (3) Proterial ML91S.

Index Terms—Automation, ferrite, high frequency (HF), core loss measurement, magnetic loss, power magnetics.

I. INTRODUCTION

✓ INIATURIZING AND IMPROVING the efficiency of power MINIATURIZING AND INTRO-LINE and electronic converters is fundamental to advancing a myriad of today's electrical systems and devices. The magnetic components in these converters currently present a critical bottleneck to improving their power density. Increasing the operating frequency of these magnetics is a ubiquitous approach to drive miniaturization, however, the benefits of doing this are strongly dependent on the loss characteristics of the core materials that comprise the magnetic component [1]-[3]. The optimal selection of material, geometry, and operating conditions are all critical for achieving the highest degree of miniaturization. Power electronic converters that have successfully achieved miniaturization utilizing medium frequency (MF) and high frequency (HF) switching operation (300kHz-30MHz)¹ include resonant inverters [4], [5], resonant dc-dc converters [6]-[8], and coupled electronic and magnetic systems (CEMS) [3], [9], [10].

One of the key challenges in the optimization of magnetic components is that their loss characteristics are highly nonlinear and inherently vary piece-to-piece owing to manufacturing imperfections. Manufacturers typically provide a set of volumetric power loss curves that are empirically fitted

¹We conform to the frequency band definitions specified by the International Telecommunications Union (ITU), where MF and HF represent the bands of the radio spectrum 300kHz-3MHz and 3MHz-30MHz, respectively.

from a relatively small data set using the Steinmetz equation [11], [12]. The loss data provided is limited and designers generally use these materials outside of their tested specifications, often attempting to extrapolate expected performance via analytical methods [13]–[15]. The most prominent methods for extrapolating magnetic loss characteristics under general operating conditions rely upon the availability of accurate sinsuoidal core loss data in the operating frequency range of interest (e.g., via the conventional Steinmetz parameters $k, \alpha,$ and β). The availability of large core loss data sets, or 'loss maps' [12], under varying operating conditions has high utility, enabling better informed magnetic component selection and subsequently optimized converter design. These large core loss data sets are also crucial for machine learning frameworks which aim to develop core loss models based upon training on large amounts of experimental measurements, such as in

Present-day electrical methods for measuring high frequency core loss under sinusoidal flux excitations [17]–[20] prove to be accurate and readily implemented, with automation of the test procedure described by the former two methods being demonstrated in [21]. The underlying issue with previous implementations of these electrical measurement methods is that they employ relatively expensive RF equipment which is designed to supply fixed resistive loads (e.g., 50Ω). Unless the equivalent resistance of the core loss testbed is actively matched to the loading requirement of the power amplifier, this equipment will present a key limitation in the ability to collect data at moderate-to-high flux density drive levels. As miniaturization efforts tend to push magnetic materials to operate at high drive levels, the inability to obtain core loss data in the regime most useful for high frequency, high performance power converter design is counter to the objectives of these testers. Since core loss is a nonlinear phenomena, the effective resistance of the magnetic component changes with drive level, therefore any power source designed to drive fixed loads without load matching capability is unsuited for these testbeds. This demonstrates a clear need for a core loss measurement method non-reliant on the traditionally employed RF power source.

To produce a core loss testing setup that is easily and inexpensively implementable in most power electronics laboratories, and to help mitigate the amplifier loading issues that limit the achievable operating range for collecting core

loss data, this work describes and verifies the suitability for a low-voltage (e.g., 100-600V) half-bridge inverter to be utilized as the driving source for 'resonant core loss testing'². Specifically, we provide an analytical framework for using the resonant quality factor Q_0 as a metric for assessing the harmonic content of the flux within the core, such that a purely sinusoidal input voltage is no longer required and a square wave excitation can be used to collect core loss data using the resonant core loss testing method described in [17], [18], [21]. This allows for the use of a simple and cost-effective switching inverter driven by a low power dc supply in lieu of the expensive arbitrary waveform generator and RF power amplifier previously utilized. Such a development is critical as it greatly simplifies the ability for researchers to obtain their own high frequency core loss data, which benefits both current large-scale core loss collection initiatives [16] and research and development of miniaturized high frequency power converters.

In Section II of this paper we describe the resonant core loss testing method which this work extends. In Section III, we provide a detailed description of the proposed core loss testing method along with an analytical framework for assessing the flux harmonics within the core solely in terms of the resonant quality factor Q_0 . In Section IV we present the hardware prototype along with experimentally collected, temperature controlled core loss data in the range 1MHz-7MHz and provide a comparison to manufacturer provided loss data. Potential error sources in the measurement procedure are also discussed. Finally, Section V concludes this paper.

II. RESONANT CORE LOSS TESTING

A. Theory of Operation

The resonant core loss testing method upon which this work is based can be understood by considering the operation of a series RLC circuit, as is shown in Fig. 1, where the RF power source is assumed to produce a purely sinusoidal voltage at the tank's resonant frequency

$$f_r = \frac{\omega_r}{2\pi} = \frac{1}{2\pi\sqrt{L_r C_r}} \tag{1}$$

Here, L_r represents the inductance of the core under test and any other equivalent series inductance (ESL) in the tank, and C_r represents a tuning capacitor utilized to achieve resonance at the desired operating frequency. It was shown in [21] that a variable vacuum capacitor is a suitable choice for providing tuning capability across a broad range of frequencies and is employed in this work. The resonant quality factor of the tank can be found as

$$Q_0 = \frac{V_{out,pk}}{V_{in,pk}} = \frac{\omega_r L_r}{R_{core} + R_{sys}}$$
 (2)

where $V_{in,pk}$ and $V_{out,pk}$ are the amplitudes of the sinusoidal input voltage and capacitor voltage, respectively, and R_{core} , R_{sus} are the effective core resistance and any other equivalent

²We use the term 'resonant core loss testing' to describe the general core loss testing method described in [17], [18], [21].

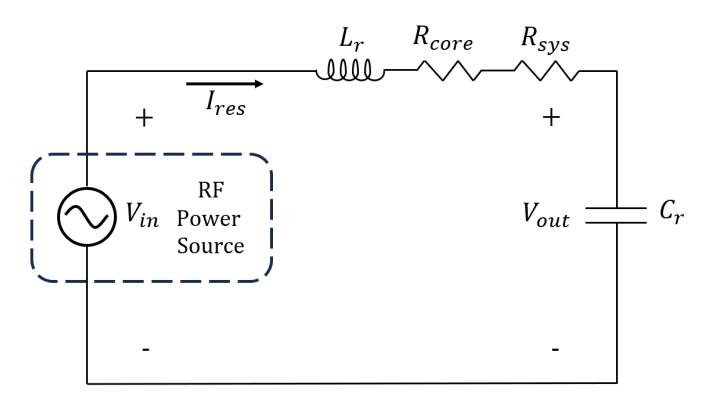


Fig. 1: Series RLC circuit fed by RF power amplifier traditionally used in 'resonant core loss testing' measurement testbeds.

series resistance (ESR) in the network (e.g., inductor winding resistance, capacitor ESR, etc.), respectively. Having premeasured R_{sys} and L_r and measuring $V_{in,pk}$ and $V_{out,pk}$ with the circuit tuned to the driving source's resonant frequency, the effective core resistance can be extrapolated by rearranging (2) as

$$R_{core} = \frac{\omega_r L_r V_{in,pk}}{V_{out,pk}} - R_{sys} \tag{3}$$

One of the primary difficulties in obtaining core loss data from this testing method is the requirement of accurate, pre-measured winding resistance values R_{cu} . In the seminal works that introduced this method [17], [18], measurement of R_{cu} was performed by constructing a coreless inductor with the same dimensions of the core to be tested and using an impedance analyzer to evaluate the resistance. In these works, it was shown via finite element analysis that the measured resistance is accurate with a magnetic core inductor for $\mu_r < 4$, but that for $\mu_r > 4$ the winding resistance could be underestimated by as much as 30% (owing to the core strongly influencing the distribution of magnetic fields around the windings, and thus their ac losses). To limit the error introduced by R_{cu} , the authors controlled the core loss to be five times larger than the copper loss.

It was shown in [21], and was employed in this work, that a less limiting approach is to use the large-signal test setup to resonate the system and take an impedance measurement at the resonant frequency. Since the impedance of a resonant tank at its resonant frequency is equal to the resistance in the system, this approach effectively measures all winding resistance and ESR without having to take discrete resistance measurements or limit the large signal operating conditions. It is noted that small signal core resistance is included in the resonant impedance measurements but is not expected to have a significant impact on the large-signal data. To reduce any error introduced by the small signal core resistance, this resistive component can be removed from the measurement via methods described in [22].

With the core resistance known, the peak sinusoidal current in the circuit at the tank's resonant frequency can be found as

$$I_{res,pk} = \frac{V_{in,pk}}{R_{core} + R_{sys}} \tag{4}$$

Noting that, at resonance, the peak capacitor voltage $V_{out,pk}$ is equal to the peak inductor voltage $V_{L,pk}$, the peak flux density is found as

$$B_{pk} = \frac{L_r I_{res,pk}}{NA_e} = \frac{V_{out,pk}}{\omega_r NA_e} \tag{5}$$

where N is the number of winding turns on the inductor and A_e is the effective cross sectional area of the magnetic core³. It is noted that (5) is only valid when functioning in the magnetic component's linear region of operation. As the magnetic cores suitable for high frequency power converters generally become considerably lossy before they reach saturation, this restraint was not limiting in this work. The volumetric power loss density can then be found as

$$P_v = \frac{I_{res,pk}^2 R_{core}}{2V_e} \tag{6}$$

where V_e is the effective volume of the core.

B. Amplifier Loading

When operating at the resonant frequency, the impedance of the RLC network is equal to the resistance in the system. It is this impedance - which generally ranges from Ω 's to tens of Ω 's for the high frequency magnetics of interest - that is seen by the output of the RF power amplifier. Commercial power amplifiers are typically linear (e.g., class A/B [23]) and are designed to be loaded by a fixed resistive load (nominally, the characteristic impedance of the system, e.g., 50Ω). Thus, [17], [18], [21] employ an impedance transformer at the input of the resonant tank to match the load to the power amplifier.

The issue with this method is that core loss is a nonlinear phenomenon, meaning that the effective resistance of the core changes with flux drive level. Therefore, as the drive level increases, the effective resistance increases, and the amplifier becomes improperly loaded. This results in a distortion of the input voltage driving the resonant tank (e.g., production of non-fundamental harmonics) and any further attempt to increase the voltage level tends to increase these harmonics rather than the fundamental of interest. The key detriment is that the amplitude of the fundamental component can no longer be appreciably increased, and subsequently neither can the flux density of interest within the core. This severely limits the utility of these methods for testing magnetic materials under high flux conditions, which prevents data collection in a regime where optimized designs may tend to push the material. It is noted that the seminal work that introduced and leveraged this testing method [17] utilized Fourier Analysis post-processing to extract the fundamental component of the

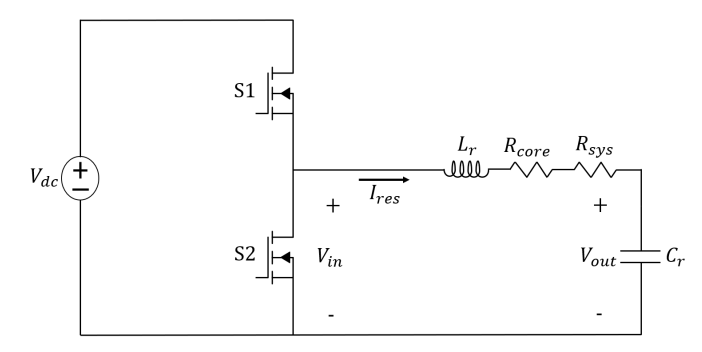


Fig. 2: Class-D amplifier circuit schematic used in the proposed core loss measurement method.

distorted input waveform due to the RF amplifier saturation. While this aids in reducing the error introduced by the generation of non-fundamental harmonics, it does not work to resolve the underlying issue of a saturated fundamental component of flux within the core.

III. CLASS-D AMPLIFIER BASED IMPLEMENTATION

A. Proposed Testing Circuit

The proposed core loss measurement circuit is a Class-D power amplifier⁴, shown in Fig. 2, where L_r is the core under test, C_r is a tuning capacitor similar to that described in Section II, and V_{dc} is a dc voltage source. The resistance R_{core} represents the effective core resistance and R_{sys} represents any other copper resistance or ESR present in the network. The half-bridge is controlled such that the switches operate in a complimentary fashion with a 50% duty cycle. The driving voltage of the series resonant tank V_{in} is therefore a square wave which varies between 0 and V_{dc} at the switching frequency f_s .

The central idea of the proposed core loss testing measurement circuit is that the resonant tank is already designed such that L_r and C_r resonate at the test frequency (which is always designed to be at the switching frequency, e.g., $f_s = f_r$) and that the resonant quality factor of the system is high $(Q_0 > 1)$, which is generally true for the low-loss inductors suitable for high frequency power converters. With the tank naturally possessing a high resonant quality factor, the core loss testing circuit can inherently filter harmonics produced by the input voltage V_{in} , which for the square wave voltage generated can be described by its Fourier Series Representation as

$$v_{in}(t) = \frac{V_{dc}}{2} + \sum_{n=odd}^{\infty} \frac{2V_{dc}}{n\pi} sin(n\omega_r t)$$
 (7)

The above features represent key advantages over the traditional power amplifier approach:

1) The fundamental component of the driving voltage is always controllable up to the limits of the dc input voltage

 $^{^3}$ It is recommended to directly measure the dimensions of the core to define A_e and V_e , as the manufacturer-provided datasheet may be different from the tested sample owing to part-to-part machining tolerances.

⁴Class-D power amplifier is the standard RF terminology for a switched mode power electronic converter that is also commonly referred to as a half-bridge resonant inverter [15].

- (whereas a power amplifier will saturate its fundamental voltage and increase harmonic levels).
- 2) The harmonics that may influence or degrade the measurement are precisely known, which is not as well described in the non-linear harmonic generation produced by a poorly loaded power amplifier.
- 3) There are many options for implementing the square wave inverter with a rating close to the expected power throughput of the test circuit (on the order of watts). In contrast, many suitable commercial RF power generators are designed to have much higher power throughputs, and this tends to make it expensive and inconvenient to source such equipment to perform this testing.

Using the Class-D amplifier shown in Fig. 2, core loss measurements can be taken in an exactly analogous fashion as was described in Section II. By replacing the amplitudes of the input and capacitor voltages $V_{in,pk}$ and $V_{out,pk}$ with the amplitudes of the fundamental components of these voltages $V_{in,1}$ and $V_{out,1}$, (2)-(6) all remain valid. This is the essence of the procedure undertaken in [17], where Fourier Analysis was performed on the input voltage in order to extract the fundamental component of the input waveform after its distortion from amplifier saturation. The main difference in this work is that the input voltage now has a considerable dc component (e.g., for the 50% duty half-bridge modulating the voltage V_{dc} , the dc component of the input voltage will be $V_{dc}/2$). This average input voltage will be blocked by the resonant capacitor, such that the peak capacitor voltage can be approximated to very high accuracy⁵ as

$$V_{out,pk} = \frac{V_{dc}}{2} + Q_0 V_{in,1}$$
 (8)

Therefore, by also extracting the fundamental component of the capacitor voltage, (2) remains valid for the resonant core loss testing measurements. This is easily verified by solving the governing equations of the series RLC circuit and/or by simulating the circuit under the requisite square wave excitations.

B. Quality Factor Measurement Metric

For the Class-D amplifier based core loss measurements to be valid, sinusoidal current must flow through the resonant tank at the test frequency of interest (as a result of the assumption of purely sinusoidal flux within the core). However, as long as this current is predominantly a single frequency sinusoid, accurate data can still be obtained by the tester. It was tacitly assumed in Section III-A that since the resonant quality factor Q_0 of the system was high, that the current harmonics would be sufficiently filtered and thus negligible to the core loss measurement. This assumption is not acceptable for the purpose of data validation. Since measuring high frequency currents to a high degree of accuracy is difficult and it is

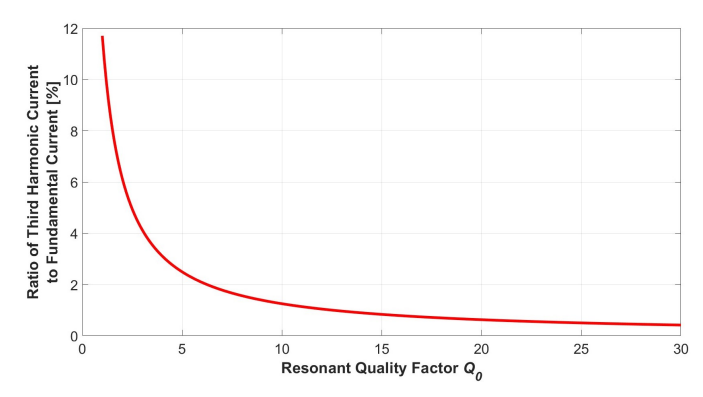


Fig. 3: Percentage of third harmonic current compared to fundamental for varying resonant quality factors.

undesirable to require measurement of many harmonics on the Fourier Spectrum in real time, a readily computable metric for determining current harmonics has high utility.

Consider that the admittance characteristics of a series resonant circuit such as in Figs. 1 and 2 can be described entirely by the resonant quality factor and the network resistance [15] as

$$Y(j\omega) = \frac{1}{R} \frac{(1/Q_0)(j\omega/\omega_r)}{(j\omega/\omega_r)^2 + (1/Q_0)(j\omega/\omega_r) + 1}$$
(9)

Taking the ratio of the admittance magnitudes at the n^{th} harmonic and at the resonant frequency then yields

$$\frac{|Y(jn\omega_r)|}{|Y(j\omega_r)|} = \frac{1}{\sqrt{1 + (Q_0 \frac{1 - n^2}{n})^2}}$$
(10)

To ensure that the n^{th} harmonic is attenuated by a factor m, the relationship

$$|Y(jn\omega_r)| \le \frac{|Y(j\omega_r)|}{m} \tag{11}$$

must be satisfied. The resonant filter is most susceptible to the 3^{rd} harmonic of the square wave input voltage (this being the largest harmonic and the closest to the resonant frequency). For the third harmonic current to be k times smaller than the fundamental current, (10) and (11) can be combined with n=3 and m=k/3 (since the 3^{rd} harmonic voltage has a magnitude 1/3 that of the fundamental for the square wave input) to produce

$$Q_0 \ge \frac{3}{8}\sqrt{\frac{k^2}{9} - 1} \tag{12}$$

The resonant quality factor's impact on 3^{rd} harmonic attenuation is plotted in Fig. 3 for quality factors between 1 and 30. The third harmonic current is less than 5% of the fundamental for $Q_0 > 2.5$, and less than 2% for $Q_0 > 6.2$, which are relatively low quality factors for high frequency resonant core loss testing. Critically, this attenuation relationship is independent of drive level if the inverter produces a square wave (or a half-wave symmetric waveshape having a 3^{rd} harmonic 1/3 or lower than the fundamental) - in contrast, an RF generator produces non-linear distortions which depend on

 $^{^5}$ The classification of an approximation here results from the omission of the small n^{th} harmonic voltage components that are present on the capacitor. This approximation has a negligible effect on the conclusions drawn from this discussion.

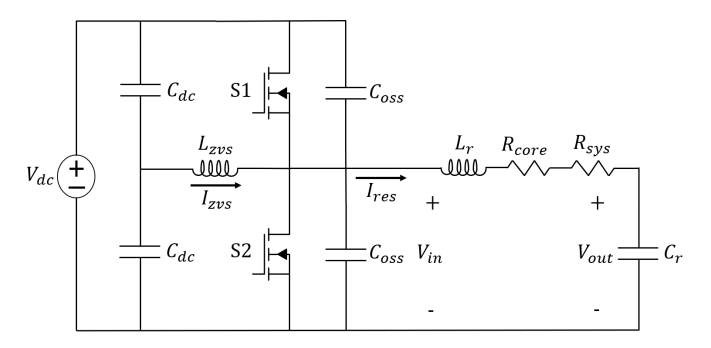


Fig. 4: ZVS assisted Class-D amplifier circuit schematic for higher power throughput core loss testing.

drive level, are inconvenient to characterize, and may be difficult to account for. Because Q_0 is already measured as part of the resonant core loss testing procedure, the proposed method also makes it convenient to automatically flag or remove data which violates any desired 3^{rd} harmonic condition.

It is important to note that the input signal to the resonant tank can be any periodic signal with a period $T_r=1/f_r$ that obeys the Dirichlet conditions [24], and hence can be described exactly by its Fourier Series Representation. It is highly advantageous to use a half-wave symmetric waveform such as a square wave so that no even harmonics are present at the input voltage, and the resonant tank will not have to filter any $2f_r$ components.

C. ZVS Assisted Implementation

With the series RLC circuit shown in Fig. 2 being tuned to resonate at the switching frequency, the tank current will be perfectly in phase with the switch node voltage. This current does not allow for zero voltage switching (ZVS) of the halfbridge switches and can prove to be insufficient for higher power core loss testing. Traditionally, the switching frequency could be altered such that it is slightly above the tanks resonant frequency, which provides a lagging current sufficient for ZVS operation of the inverter switches, but since the tank must always be tuned to resonate at the switching frequency for this implementation, ZVS is not achievable in this manner. To provide ZVS of the half-bridge switches and allow for higher power throughput during core loss testing, the measurement circuit in Fig. 2 can be altered such as is shown in Fig. 4, where C_{oss} represents the linearized time-equivalent capacitance of the inverter switches [25], L_{zvs} is a ZVS assisting inductor, and the capacitors C_{dc} are dc link capacitors to stabilize the voltage across L_{zvs} . Since L_{zvs} provides the necessary current for ZVS of the inverter switches, the resonant tank does not require inductive tuning and the core loss testing method outlined in Section III-A can be carried out as described. A more detailed discussion on the operation of this circuit is provided in [15].

The primary difficulty with this circuit implementation is that the parasitic output capacitance of the inverter switches is a nonlinear function of the drain-to-source voltage and

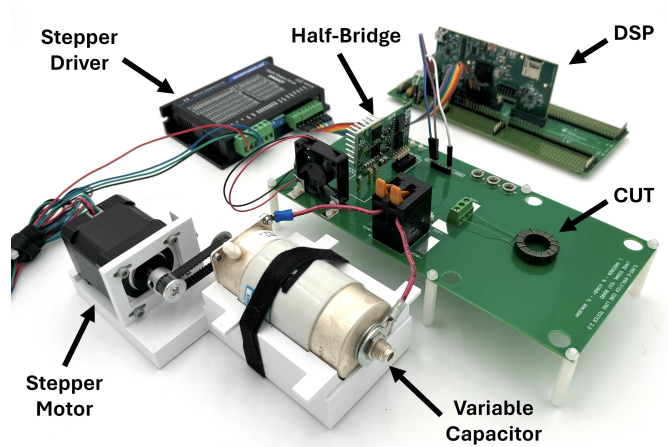


Fig. 5: Class-D amplifier based core loss testing experimental prototype. The half-bridge module shown is Texas Instruments LMG3410-HB-EVM.

TABLE I: Prototype components and instrumentation

Equipment	Manufacturer	Model
DC Power Supply	Keithley	2230-60-3
Half-Bridge Module 1	Texas Instruments	LMG3410-HB-EVM
Half-Bridge Module 2	On Semiconductor	NCP51810GAN1GEVB
Microcontroller	Texas Instruments	TMS320C2000
Digital Oscilloscope	Tektronix	MSO44
High Voltage Probe	Tektronix	TPP0850
Low Voltage Probe	Tektronix	TPP1000
Thermal Cooling Unit	ThermoStream	TP04100A
Impedance Analyzer	Omicron Lab	Bode100
Variable Capacitor	Jennings	CMV1-1000-0303
Stepper Motor	StepperOnline	17HS19-200451
Stepper Driver	StepperOnline	DM542T

therefore the deadtime required to charge and discharge these capacitors for ZVS operation varies with the dc voltage driving the system. To avoid long intervals of reverse conduction, the deadtime should be actively changed to satisfy the following⁶

$$dt = 16f_s L_{zvs} C_{oss}(V_{dc}) \tag{13}$$

where the dependence of the output capacitance on the dc input voltage is by virtue of the dependence on the drain-to-source blocking voltage of the inverter switches. While the bulk core loss data in this paper was not generated using this implementation, a prototype was implemented to validate the above discussion, as is discussed in further detail in Section IV.

IV. RESULTS AND MANUFACTURER DATA COMPARISON

A. Class-D Amplifier Experimental Prototype

The experimental prototype for the Class-D amplifier-based core loss tester without auxiliary ZVS circuitry is shown

⁶The linearized time-equivalent capacitance should be used in (13). For situations where it is impractical to determine this value, the charge-equivalent capacitance remains a good approximation since the inductor current is roughly constant during the switching transition [25].

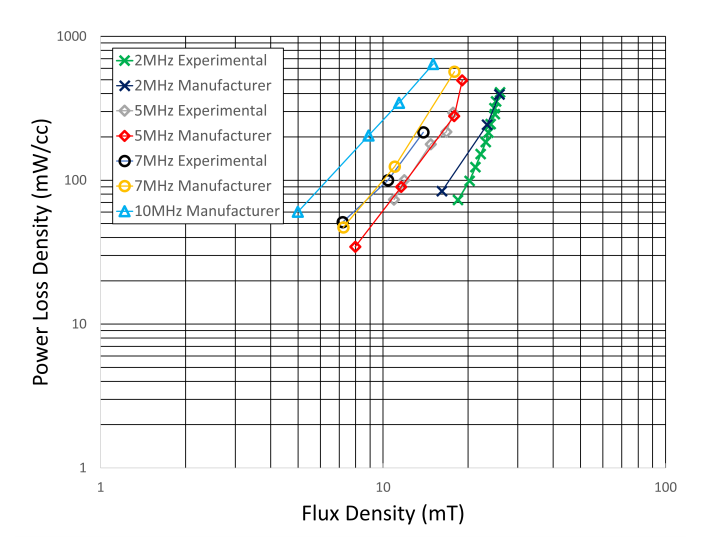


Fig. 6: Comparison of experimentally collected and manufacturer reported core loss data from 2-7MHz at 25°C using the Class-D amplifier based core loss measurements for Fair-Rite 67 NiZn material.

in Fig. 5, where the voltage probes and temperature control solution are not included in the figure for clarity. The equipment and instrumentation utilized in this prototype are provided in Table I. The stepper motor and variable capacitor are controlled using the DSP to tune the circuit to the testing resonant frequency. Two separate off-the-shelf half-bridge modules were tested in this prototype, with the LMG3410-HB-EVM and NCP51810GAN1GEVB proving suitable for up to 2MHz and 10MHz operation, respectively.

While not the focus of this paper, it is of note that an automation system was developed for this experimental prototype using Python to control all of the test and measurement equipment. The automation procedure is similar in scope to that described in [21]. A temperature control solution was also used in this work, with the ThermoStream TP04100A providing chilled air to regulate the core temperature during testing. Further details on the implementation of the thermal control can be found in [26].

B. Experimental Data

Experimentally collected core loss data for Fair-Rite 67 material in the range 2-7MHz, Fair-Rite 80 material in the range 1-2MHz, and Proterial ML91S material in the range 1-2MHz is shown in Figs. 6-8 along with manufacturer reported data. The lowest resonant quality factor Q_0 observed for Fair-Rite 67, Fair-Rite 80, and Proterial ML91S data provided is 26.2, 14.4, and 17.1, respectively, corresponding to a third harmonic current flow that is 0.48%, 0.87%, and 0.73% of the fundamental current. These third harmonic current flows are negligible and the tank current is approximately a pure tone, providing high confidence in the data collected. The loss data for Fair-Rite 67 and Fair-Rite 80 was collected on toroidal cores with dimensions 22.1mm, 13.7mm, 6.35mm

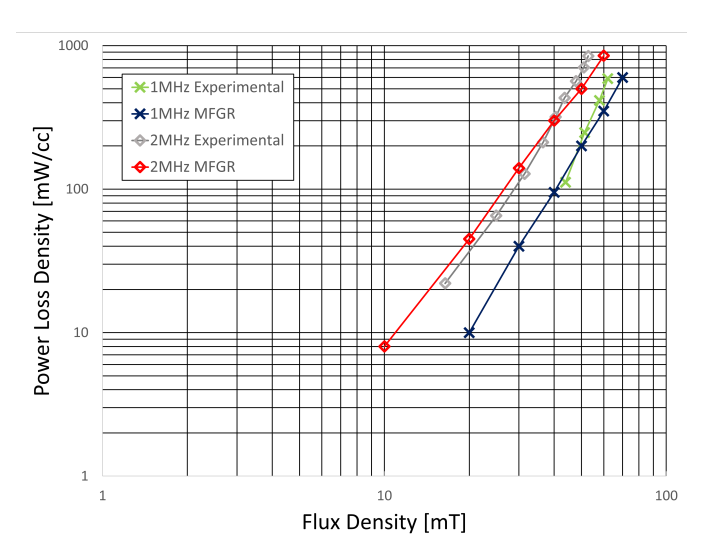


Fig. 7: Comparison of experimentally collected and manufacturer reported core loss data from 1-2MHz at 25°C using the Class-D amplifier based core loss measurements for Fair-Rite 80 MnZn material.

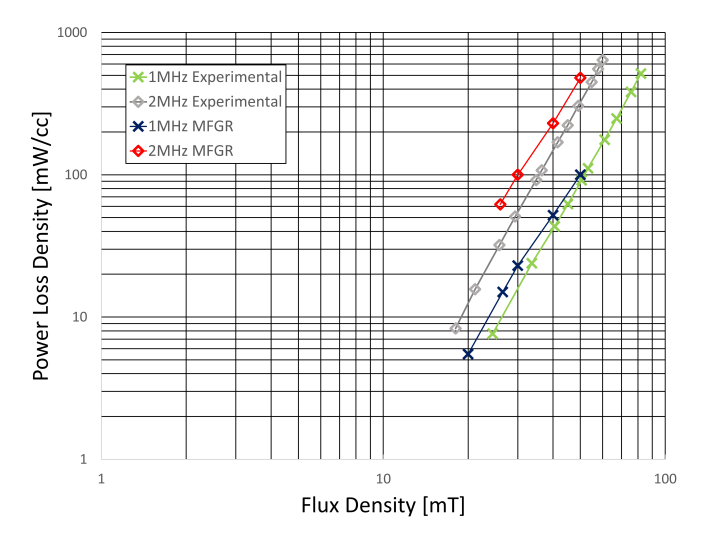


Fig. 8: Comparison of experimentally collected and manufacturer reported core loss data from 1-2MHz at 25°C using the Class-D amplifier based core loss measurements for Proterial ML91S MnZn material.

and Proterial ML91S data was collected on an EIR core with dimensions 25mm, 8mm, 14.8mm. All reported data was collected at a temperature of 25°C. Fig. 9 shows an example operating waveform for a loss point collected with $Q_0 \approx 29$.

C. Potential Error Sources

1) Resistance Measurement: The measurement accuracy of resonant core loss testing is highly dependent on possessing high quality system resistance measurements (e.g., winding resistance, capacitor ESR, etc.). These resistance measurements are directly utilized in the calculation of effective core resistance and peak ac current and subsequently have a

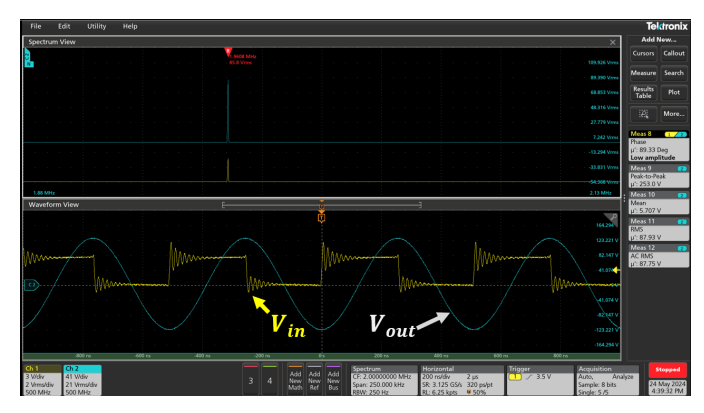


Fig. 9: Example operating waveform capture at resonance for 2MHz FR80 core loss sample point.

profound impact on the estimated flux density and power loss in the core. In this work, the system resistance was measured by taking impedance measurements with the circuit tuned to resonance. This method inherently compensates for any system resistance which would not otherwise be easily measured (e.g., trace resistance on the printed circuit board, terminal contact resistance, etc.) but fails to extract small signal core ESR. The additional small signal core resistance measured manifests itself as an underestimate in peak ac current and an overestimate in the core resistance. Since the small signal core resistance is expected to be much smaller than the system resistances measured, it is likely that small errors are present in the data collected, with an amplification of these errors at low drive levels. While not executed in this work, methods exist for extracting small signal core resistance from impedance measurements [22] and the impact of this measurement will be explored in future work.

2) Resonant Point and Winding Capacitance: For core materials suitable for high frequency power conversion, the quality factor of the core under test is generally very high (up to $Q_0 = 350$ observed in this work). While this is beneficial for filtering harmonics produced by the square wave input, the resonant peaks become increasingly sharp and finding the exact resonant point requires very high granularity in the installed capacitance. The stepper motor and variable capacitor employed in this work provide an achievable resolution under 0.1 pF which allows for high precision in the resonant tuning. It was observed during testing that this high precision remained insufficient at particular operating conditions and the exact resonant point was unachievable, resulting in errors in the estimated quality factor and subsequently the extrapolated core resistance. To combat this issue, additional winding turns were added for the purpose of decreasing the quality factor of the core under test. This aided in damping the system to find the desired resonant point but affects its selfresonant frequency and degrades the small signal impedance measurements⁷. It was found in simulation that controlling the self resonant frequency of the core under test to be an order of magnitude larger than the operating point of interest yielded negligible (i.e., <1%) effects on the impedance measurement. All of the data presented in this paper was gathered on cores that met this criterion.

D. ZVS Assisted Implementation

The power throughput observed during collection of the data presented in Section IV-B (approximately 5W of core loss) was not large enough to require ZVS of the inverter switches. While the data presented in this paper was not collected under the implementation described in Section III-C, the circuit of Fig. 4 was designed and implemented to validate the modeling discussed. The ZVS assist inductor L_{zvs} was implemented as a 30nH air-core inductor using 16AWG solid copper wound on a 3D-printed bobbin. Sample loss data points taken with this implementation are consistent with those collected using the prototype in Fig. 5.

V. CONCLUSION

This work proposes a Class-D power amplifier-based magnetic core loss tester developed for 100kHz-10MHz measurements. A comprehensive overview of the proposed measurement circuit is provided and an analytical framework for assessing flux harmonics within the core via peak voltage measurements is developed. The experimental prototype is presented and power loss data sets are provided for Fair-Rite 67, Fair-Rite 80, and Proterial ML91S materials in the range 1-7MHz. Potential error sources are discussed and opportunities for optimizing the accuracy of the tester are proposed. Future work will seek to develop a large-scale open source core loss data base for high frequency magnetic materials across a broad range of frequencies and flux densities.

VI. ACKNOWLEDGMENTS

The authors would like to thank Proterial (formerly Hitachi Metals) for providing ML91S core samples, Mr. Erik Rodriguez for designing and implementing the motor driven variable capacitor, and Mr. Emmanuel Havugimana for valuable input on using Python for automation.

REFERENCES

- [1] D. J. Perreault, J. Hu, J. M. Rivas, Y. Han, O. Leitermann, R. C. Pilawa-Podgurski, A. Sagneri, and C. R. Sullivan, "Opportunities and challenges in very high frequency power conversion," in 2009 Twenty-Fourth Annual IEEE Applied Power Electronics Conference and Exposition, 2009, pp. 1–14.
- [2] C. R. Sullivan, B. A. Reese, A. L. F. Stein, and P. A. Kyaw, "On size and magnetics: Why small efficient power inductors are rare," in 2016 International Symposium on 3D Power Electronics Integration and Manufacturing (3D-PEIM), 2016, pp. 1–23.
- [3] M. K. Ranjram and D. J. Perreault, "A 380-12 v, 1-kw, 1-mhz converter using a miniaturized split-phase, fractional-turn planar transformer," *IEEE Transactions on Power Electronics*, vol. 37, no. 2, pp. 1666–1681, 2022

⁷Increasing the winding capacitance of an inductor can significantly increase the small signal impedance measurements taken on an impedance analyzer [22].

- [4] J. M. Rivas, Y. Han, O. Leitermann, A. D. Sagneri, and D. J. Perreault, "A high-frequency resonant inverter topology with low-voltage stress," *IEEE Transactions on Power Electronics*, vol. 23, no. 4, pp. 1759–1771, 2008.
- [5] J. Choi, D. Tsukiyama, Y. Tsuruda, and J. M. R. Davila, "High-frequency, high-power resonant inverter with egan fet for wireless power transfer," *IEEE Transactions on Power Electronics*, vol. 33, no. 3, pp. 1890–1896, 2018.
- [6] J. Hu, A. D. Sagneri, J. M. Rivas, Y. Han, S. M. Davis, and D. J. Perreault, "High-frequency resonant sepic converter with wide input and output voltage ranges," *IEEE Transactions on Power Electronics*, vol. 27, no. 1, pp. 189–200, 2012.
- [7] P. Shamsi and B. Fahimi, "Design and development of very high frequency resonant dc-dc boost converters," *IEEE Transactions on Power Electronics*, vol. 27, no. 8, pp. 3725–3733, 2012.
- [8] A. Nabih and Q. Li, "A method to embed resonant inductor into pcb matrix transformer for high-density resonant converters," *IEEE Transactions on Power Electronics*, vol. 39, no. 2, pp. 2385–2400, 2024.
- [9] M. K. Ranjram, I. Moon, and D. J. Perreault, "Variable-inverter-rectifier-transformer: A hybrid electronic and magnetic structure enabling adjustable high step-down conversion ratios," *IEEE Transactions on Power Electronics*, vol. 33, no. 8, pp. 6509–6525, 2018.
- [10] M. K. Ranjram and D. J. Perreault, "Leveraging multi-phase and fractional-turn integrated planar transformers for miniaturization in data center applications," in 2020 IEEE 21st Workshop on Control and Modeling for Power Electronics (COMPEL), 2020, pp. 1–8.
- [11] C. P. Steinmetz, "On the law of hysteresis," *Transactions of the American Institute of Electrical Engineers*, vol. IX, no. 1, pp. 1–64, 1892.
- [12] E. Herbert, "Psma-sma phase ii project: Generic specification for ferrite cores." 2017.
- [13] K. Venkatachalam, C. Sullivan, T. Abdallah, and H. Tacca, "Accurate prediction of ferrite core loss with nonsinusoidal waveforms using only steinmetz parameters," in 2002 IEEE Workshop on Computers in Power Electronics, 2002. Proceedings., 2002, pp. 36–41.
- [14] M. Mu and F. C. Lee, "A new core loss model for rectangular ac voltages," in 2014 IEEE Energy Conversion Congress and Exposition (ECCE), 2014, pp. 5214–5220.
- [15] J. G. Kassakian, D. J. Perreault, G. C. Verghese, and M. F. Schlect, Principles of Power Electronics, 2nd ed. New York: Cambridge University Press, 2023.
- [16] H. Li, S. R. Lee, M. Luo, C. R. Sullivan, Y. Chen, and M. Chen, "Magnet: A machine learning framework for magnetic core loss modeling," in 2020 IEEE 21st Workshop on Control and Modeling for Power Electronics (COMPEL), 2020, pp. 1–8.
- [17] Y. Han, G. Cheung, A. Li, C. R. Sullivan, and D. J. Perreault, "Evaluation of magnetic materials for very high frequency power applications," *IEEE Transactions on Power Electronics*, vol. 27, no. 1, pp. 425–435, 2012.
- [18] A. J. Hanson, J. A. Belk, S. Lim, C. R. Sullivan, and D. J. Perreault, "Measurements and performance factor comparisons of magnetic materials at high frequency," *IEEE Transactions on Power Electronics*, vol. 31, no. 11, pp. 7909–7925, 2016.
- [19] M. Mu, Q. Li, D. J. Gilham, F. C. Lee, and K. D. T. Ngo, "New core loss measurement method for high-frequency magnetic materials," *IEEE Transactions on Power Electronics*, vol. 29, no. 8, pp. 4374–4381, 2014.
- [20] D. Hou, M. Mu, F. C. Lee, and Q. Li, "New high-frequency core loss measurement method with partial cancellation concept," *IEEE Transactions on Power Electronics*, vol. 32, no. 4, pp. 2987–2994, 2017.
- [21] J. R. Anderson and M. K. Ranjram, "Automation of high-frequency magnetic core loss data collection," in 2023 IEEE 24th Workshop on Control and Modeling for Power Electronics (COMPEL), 2023, pp. 1– 8.
- [22] B. X. Foo, A. L. F. Stein, and C. R. Sullivan, "A step-by-step guide to extracting winding resistance from an impedance measurement," in 2017 IEEE Applied Power Electronics Conference and Exposition (APEC), 2017, pp. 861–867.
- [23] Model 150A100D Operating and Service Manual, AR RF/Microwave Instrumentation, 2018. [Online]. Available: https://arworld.us/ wp-content/uploads/2021/12/150A100D_Manual-Rev-A.pdf
- [24] A. V. Oppenheim and S. Willsky, Alan, Signals and Systems, 2nd ed. New Jersey: Prentice Hall, 1996.
- [25] D. Costinett, D. Maksimovic, and R. Zane, "Circuit-oriented treatment of nonlinear capacitances in switched-mode power supplies," *IEEE Transactions on Power Electronics*, vol. 30, no. 2, pp. 985–995, 2015.

[26] N. J. Kirkby and M. K. Ranjram, "Temperature control for automated high frequency core loss testing," in 2024 IEEE 25th Workshop on Control and Modeling for Power Electronics (COMPEL), 2024, pp. 1–8.